23rd ABCM International Congress of Mechanical Engineering
December 6-11, 2015, Rio de Janeiro, RJ, Brazil

BUCKLING AND NONLINEAR VIBRATIONS ANALYSIS OF CONOIDAL SHELLS

Renata M. Soares
Federal University of Goiás, av. Universitária no. 1488, 74605-220, Goiânia, Goiás.
msrenata@gmail.com

Paulo B. Gonçalves
Pontifical Catholic University of Rio de Janeiro, av. Marquês de São Vicente no. 225, 22451-900, Rio de Janeiro, RJ.
paulo@puc-rio.br

Abstract. *Slender shell structures described by ruled surfaces have been frequently used in civil engineering and among these slender shells, conoidal shells are frequently favored as roofing units to cover large column-free areas due to the ease of construction, aesthetic value and structural efficiency. This work studies the nonlinear buckling behavior and the linear and nonlinear free vibration response of a conoidal shell, using commercial finite element software ABAQUS®. The problem is geometrically nonlinear due to the shell strong geometric nonlinearity, especially in the case of shallow shells used in practical applications. The results show the influence of the geometry on the nonlinear response, buckling loads, linear natural frequencies, vibration modes and nonlinear frequency-amplitude relation.*

Keywords: *Conoidal shells, nonlinear vibration analysis, ruled surfaces, buckling behavior*

1. INTRODUCTION

The structural behavior of conoidal shells is a problem of relevance in civil engineering, as they are frequently used in modern shell roof structures because of their architectural aesthetics and functional requirements. The conoidal shell structures are described by ruled surfaces and they are one of the most economical structural solutions to cover large spans (Linkwitz, 1999). Ruled surfaces are obtained by the movement of one or more straight lines along one or more curves. So they are easy to cast, which justifies their choice in many cases. For aesthetic and structural reasons these structures are usually shallow surfaces, which leads, as in the case of shallow arches, to a strong geometric nonlinearity. Furthermore, the conoidal shells have a preference in the industry because these shell forms are singly ruled surfaces which can be generated by placing straight shuttering between two curved boundaries in the opposite edges.

Several papers deal with the structural analysis of conoidal shells. For example, Ghosh and Bandyopadhyay (1990) analyzed approximately the bending of conoidal shells using the Galerkin method. Later Das and Bandyopadhyay (1993) compared the numerical finite element results with the experimental results obtained for a conoidal concrete shell. Nayak and Bandyopadhyay (2002) investigated, using the finite element method, the free vibrations of stiffened conoidal shells while Balkshi and Chakravorty (2014) studied the first ply failure of thin composite conoidal shells subjected to uniformly distributed loads. Recently, Cavalcanti and Gonçalves (2014) studied the buckling and vibration characteristics of conoidal shell through a detailed parametric analysis to understand the influence of boundary conditions and different spans on their structural behavior.

In the present work the linear and nonlinear buckling behavior and the linear and nonlinear free vibration response of a conoidal shell is investigated, using commercial finite element software ABAQUS®. This problem has not been tackled in the technical literature and it is important for a safe and economical design. The results show the strong influence of the boundary conditions, shell curvature and geometric nonlinearity on the nonlinear response, natural frequencies and buckling loads.

2. MATHEMATICAL FORMULATION

Consider a conoidal shell of high arch height H_h, lower arch height H_l, thickness h, length a and width $2b$, made of a linear elastic material with Young's modulus E, Poisson coefficient υ and mass density ρ, as illustrated in Fig. 1.

The surface of a truncated parabolic conoid is described by (Ghosh and Bandyopadhyay, 1990):

$$z(x,y) = -H_h\left[1-\left(1-\frac{H_l}{H_h}\right)\frac{x}{a}\right]\left[1-\frac{y^2}{b^2}\right] \tag{1}$$

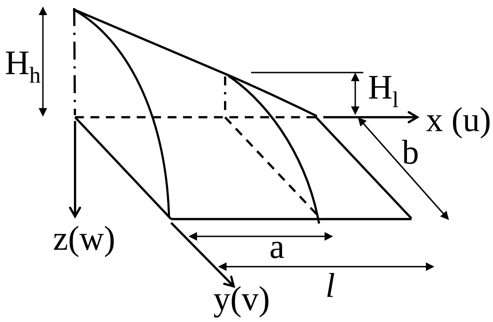

Figure 1. Geometry of the truncated parabolic conoid (half shell).

The vertical load per unit horizontal area of the shell surface is given by:

$$\bar{q} = q\left[1+\left(\frac{\partial z(x,y)}{\partial x}\right)^2+\left(\frac{\partial z(x,y)}{\partial y}\right)^2\right]^{1/2} \tag{2}$$

where q is the magnitude of the gravitational load distributed on the shell surface.

Considering the shallow curved surface, the z-displacement component at any point can be written as (Ghosh and Bandyopadhyay, 1990):

$$\overline{w} = w + z(x,y) \tag{3}$$

Therefore, the strain-displacement relations for the conoidal shell middle surface, rotations and changes of curvature can be written based on von Kármán plate theory, as (Brush and Almroth, 1975):

$$\begin{aligned} &\varepsilon_x = u_{,x} + \frac{1}{2}(w_{,x}^2 + 2w_{,x}z_{,x}) \qquad \varepsilon_y = v_{,y} + \frac{1}{2}(w_{,y}^2 + 2w_{,y}z_{,y}) \qquad \gamma_{xy} = u_{,x} + v_{,x} + w_{,x}w_{,y} + w_{,x}z_{,y} + w_{,y}z_{,x} \\ &\kappa_x = -w_{,xx} \qquad \kappa_y = -w_{,yy} \qquad \kappa_{xy} = w_{,xy} \end{aligned} \tag{4}$$

The conoidal shell deformations $\left(\bar{\varepsilon}_x, \bar{\varepsilon}_\theta \text{ and } \bar{\gamma}_{x\theta}\right)$ at an arbitrary point are given in terms of these middle surface strains and changes of curvature by:

$$\bar{\varepsilon}_x = \varepsilon_x + z\kappa_x \qquad \bar{\varepsilon}_y = \varepsilon_y + z\kappa_y \qquad \bar{\gamma}_{xy} = \gamma_{xy} + 2z\kappa_{xy} \tag{5}$$

For an isotropic, elastic material the stress components, at an arbitrary point along the shell thickness, are given by:

$$\begin{Bmatrix} \bar{\sigma}_x \\ \bar{\sigma}_\theta \\ \bar{\tau}_{x\theta} \end{Bmatrix} = \frac{E}{(1-\upsilon^2)}\begin{bmatrix} 1 & \upsilon & 0 \\ \upsilon & 1 & 0 \\ 0 & 0 & \frac{(1-\upsilon)}{2} \end{bmatrix}\begin{Bmatrix} \bar{\varepsilon}_x \\ \bar{\varepsilon}_\theta \\ \bar{\gamma}_{x\theta} \end{Bmatrix} \tag{6}$$

The force and moments resultants are obtained by the integration of the stress components along the conoidal shell thickness as follows:

$$\begin{aligned} &N_x = \int_{-h/2}^{h/2} \bar{\sigma}_x\, dz \qquad N_y = \int_{-h/2}^{h/2} \bar{\sigma}_y\, dz \qquad N_{xy} = \int_{-h/2}^{h/2} \bar{\tau}_{xy}\, dz \\ &M_x = \int_{-h/2}^{h/2} \bar{z}\,\bar{\sigma}_x\, dz \qquad M_y = \int_{-h/2}^{h/2} \bar{z}\,\bar{\sigma}_y\, dz \qquad M_{xy} = \int_{-h/2}^{h/2} \bar{z}\,\bar{\tau}_{xy}\, dz \end{aligned} \tag{7}$$

Therefore, the equilibrium equations having as a reference the center of the shell are given by:

$$u_{,xx}+H_h\frac{g}{a}\left(1-\frac{y^2}{b^2}\right)w_{,xx}+\nu\left(v_{,xy}-2H_h\frac{g}{a}\frac{y}{b^2}w_{,y}+2H_h\frac{y}{b^2}\left(1-g\frac{2x+a}{2a}\right)w_{,xy}\right)+$$
$$\frac{1-\nu}{2}\left(\begin{array}{l}u_{,yy}+v_{,xy}+2H_h\frac{y}{b^2}\left(1-g\frac{2x+a}{2a}\right)w_{,xy}+2H_h\frac{1}{b^2}\left(1-g\frac{2x+a}{2a}\right)w_{,x}+2H_h\frac{g}{a}\frac{y}{b^2}w_{,y}\\+H_h\frac{g}{a}\left(1-\frac{y^2}{b^2}\right)w_{,yy}\end{array}\right)=0 \tag{8}$$

$$v_{,yy}+2H_h\left(1-g\frac{2x+a}{2a}\right)\left(\frac{w_{,y}}{b^2}+\frac{y\,w_{,yy}}{b^2}\right)+\nu\left(u_{,xy}-2H_h\frac{g}{a}\frac{y}{b^2}w_{,x}+H_h\frac{g}{a}\left(1-\frac{y^2}{b^2}\right)w_{,xy}\right)+$$
$$\frac{1-\nu}{2}\left(u_{,xy}+v_{,xx}+2H_h\frac{y}{b^2}\left(1-g\frac{2x+a}{2a}\right)w_{,xx}-2H_h\frac{g}{a}\frac{y}{b^2}\;w+H_h\frac{g}{a}\left(1-\frac{y^2}{b^2}\right)w_{,yx}\right)=0 \tag{9}$$

$$D\nabla^4w-(1-\nu)C\left[-2H_h\frac{g}{a}\frac{y}{b^2}(u_{,y}+v_{,x}+2H_h\frac{y}{b^2}\left(1-g\frac{2x+a}{2a}\right)w_{,x}+H_h\frac{g}{a}\left(1-\frac{y^2}{b^2}\right)w_{,y})\right]$$
$$-C\left[2H_h\frac{1}{b^2}\left(1-g\frac{2x+a}{2a}\right)(v_{,y}+2H_h\frac{y}{b^2}\left(1-g\frac{2x+a}{2a}\right)w_{,y}+\nu\,u_{,x}+H_h\frac{g}{a}\left(1-\frac{y^2}{b^2}\right)w_{,x})\right]$$
$$+\rho\,h\,\ddot{w}=q\left[1+\left(H_h\frac{g}{a}\left(1-\frac{y^2}{b^2}\right)\right)^2+\left(2H_h\frac{y}{b^2}\left(1-g\frac{2x+a}{2a}\right)\right)^2\right]^{1/2} \tag{10}$$

where $C = E\,h/(1-\upsilon^2)$ and $D = E\,h^3/12(1-\upsilon^2)$ are, respectively, the extensional and flexural shell stiffness parameters, and $g = 1-(H_l/H_h)$.

3. NUMERICAL RESULTS

Consider an incomplete concrete conoidal shell with thickness $h = 6$cm and the following dimension $a = 6$ *m*, $2b = 8$ *m*, H_h = variable and $H_l = 0.5\,H_h$ (see Fig. 1). The material properties are: Young's modulus $E = 14$ GPa; Poisson ratio $\nu = 0.30$ and weight density $\rho = 25$ kN/m^3. Different boundary conditions are prescribed along the two straight boundaries of the conoidal shell: (1) the two straight boundaries are clamped (CC) and (2) the two straight boundaries are simply-supported (SS). The two curved boundaries are free, a usual boundary condition in most applications.

In order to get the linear and non-linear results, the finite element software ABAQUS® is used. Convergence of the results can be obtained using the shell element S4R and a mesh of elements with plane lengths $l_x = 0.1$ and $l_y = 0.16$.

3.1 Linear results

Since the shell geometry and loading is symmetric with respect to the *x* axis (see Fig. 1), the initial deformation pattern of the shell is symmetric. However, as in the case of an arch, the buckling mode can be symmetric or asymmetric. Thus, two cases are considered in the linear buckling analysis. First the complete shell is discretized using the FEM and the critical load is obtained (q_{cr}), and then only half shell is considered, imposing the proper symmetry constraints at *y*=0 and the associated critical load (q_{crsy}) is obtained. The two buckling loads are shown in Table 1 for five values of the shell height H_h and the two sets of boundary conditions. Also shown in Table 1 are the three lowest natural frequencies of the unloaded shell. In all cases q_{crsy} is much higher than q_{cr}, increasing this difference with H_h. Also the results for the clamped shell (CC) are, as expected, much higher than those for the simply-supported shell (SS) demonstrating the importance of the boundary conditions on the shell load carrying capacity. Thus the results show that for the geometries considered in this work the buckling mode is always asymmetric. Also the lowest natural frequency is associated with an asymmetric mode. Again, the natural frequencies for the simply-supported shell are lower than those for the clamped shell. The buckling modes and the three lowest vibrations modes of the conoidal shell with $H_h = 1.5$ are shown in Fig. 2 and Fig. 3, respectively. The other geometries display similar deformation patterns.

Since the conoidal shell has an eminently nonlinear behavior under gravitational loading, the linear eigenvalue buckling problem gives only an approximate estimation of the critical load, as will be shown by the nonlinear analysis. A better estimation could be obtained using a quadratic eigenvalue problem, but its solution is usually rather cumbersome (Tisseur and Meerbergen, 2001).

Table 1: Buckling loads and natural frequencies for different conoidal shells geometries.

Boundary conditions	H_h (m)	q_{cr} (kPa)	q_{crsy} (kPa)	ω_1 (rad/s)	ω_2 (rad/s)	ω_3 (rad/s)
CC	0.5	15.006	21.989	42.042	63.434	67.376
CC	1.0	29.147	81.101	41.998	69.301	79.929
CC	1.5	43.209	134.68	41.267	66.148	81.743
CC	2.0	55.663	175.80	39.764	61.056	81.622
CC	2.5	66.220	199.48	37.839	55.649	80.749
SS	0.5	7.999	21.989	28.615	53.557	62.033
SS	1.0	17.719	59.272	30.081	52.674	68.010
SS	1.5	28.525	98.149	30.753	49.657	70.784
SS	2.0	38.580	127.54	30.473	45.533	72.079
SS	2.5	46.800	134.77	29.512	41.214	72.266

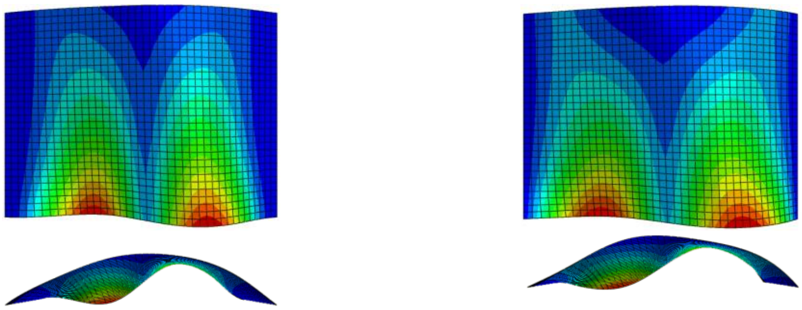

(a) (b)

Figure 2. Buckling modes of conoidal shell: (a) clamped and (b) simply-supported. H_h =1.5m.

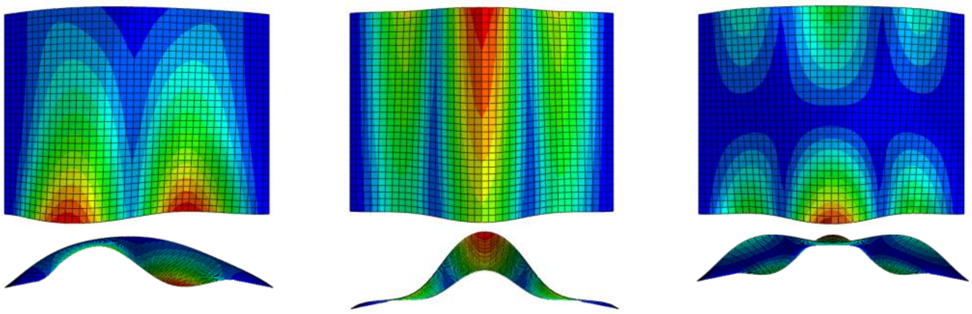

1st mode 2nd mode 3rd mode

(a)

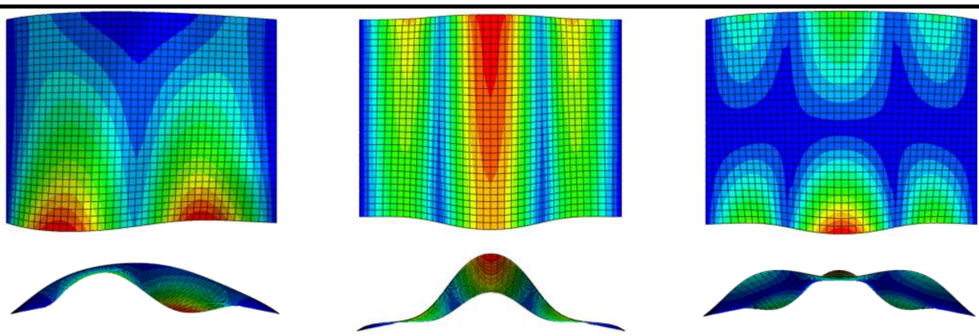

1st mode 2nd mode 3rd mode

(b)

Figure 3. Vibration modes of the conoidal shell: (a) clamped (b) simply-supported. H_h =1.5m.

3.2 Nonlinear analysis

The nonlinear equilibrium path is obtained using the finite element method. The results are shown in Fig. 4 for a clamped conoidal shell and in Fig. 5 for a simply-supported shell. In these figures the load magnitude (see Eq. 2) is plotted as a function of transversal displacement in a point with coordinates $(x, y) = (3, 0)$ considering, as in the linear case, two FE models: the full shell (black path) and half shell (symmetric case – blue path). The dots along the vertical axis correspond to the linear buckling load (BL) presented in Tab.1. As the load increases the effective stiffness decreases and becomes zero at the first load limit point, where the shell loses its stability. After this, the shell displays highly nonlinear equilibrium paths with several load and displacement limit points. As observed here, the linear stability analysis either overestimates or underestimates the buckling load obtained by the nonlinear analysis. Thus, for this class of shell structures buckling loads obtained through a linear analysis may lead to erroneous results. However, the nonlinear analysis confirms that buckling occurs in an asymmetric mode at load levels much lower than that obtained through a symmetric mode.

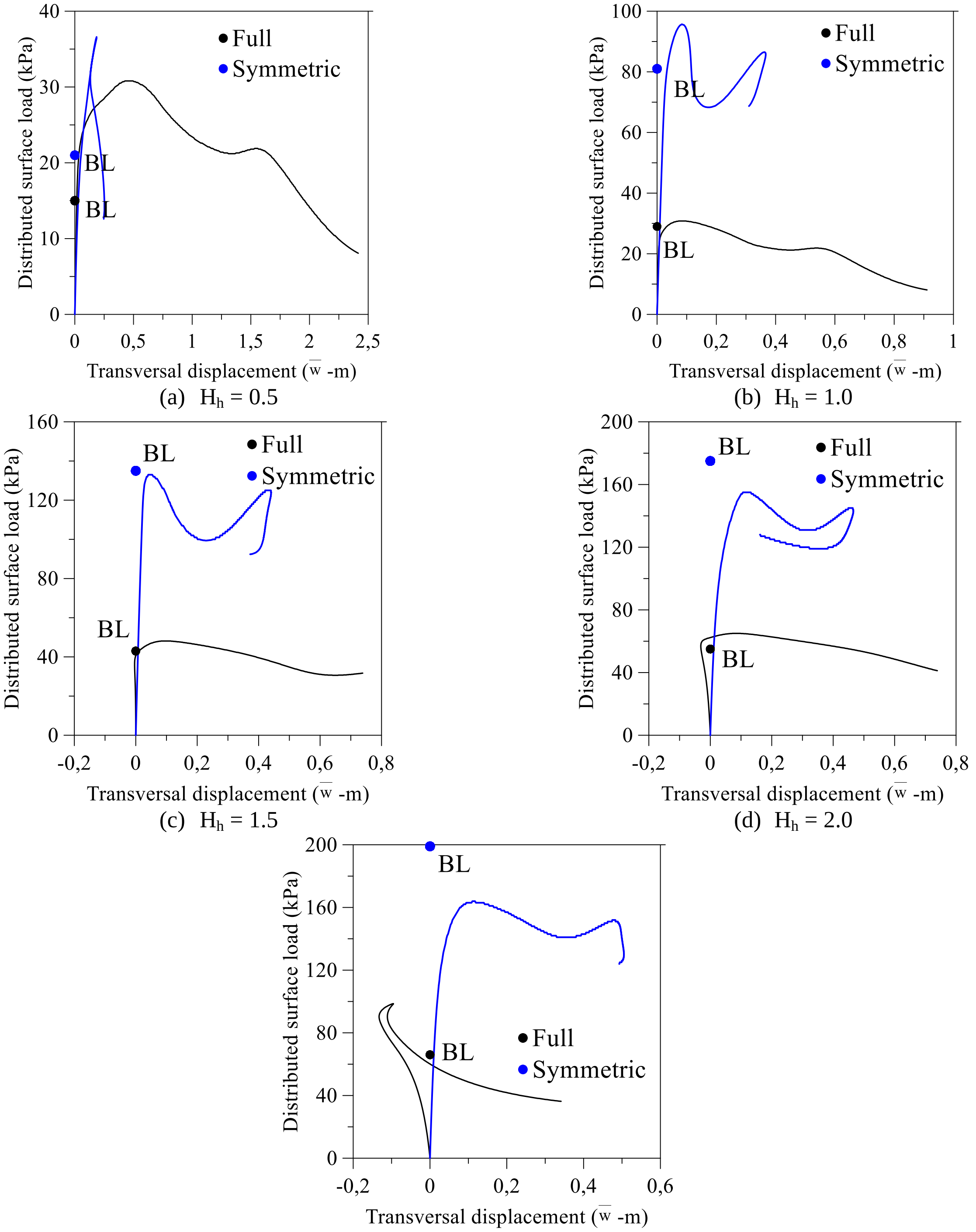

(a) $H_h = 0.5$ (b) $H_h = 1.0$ (c) $H_h = 1.5$ (d) $H_h = 2.0$ (e) $H_h = 2.5$

Figure 4. Nonlinear equilibrium paths for a clamped conoidal shell. Point $(x, y) = (3,0)$

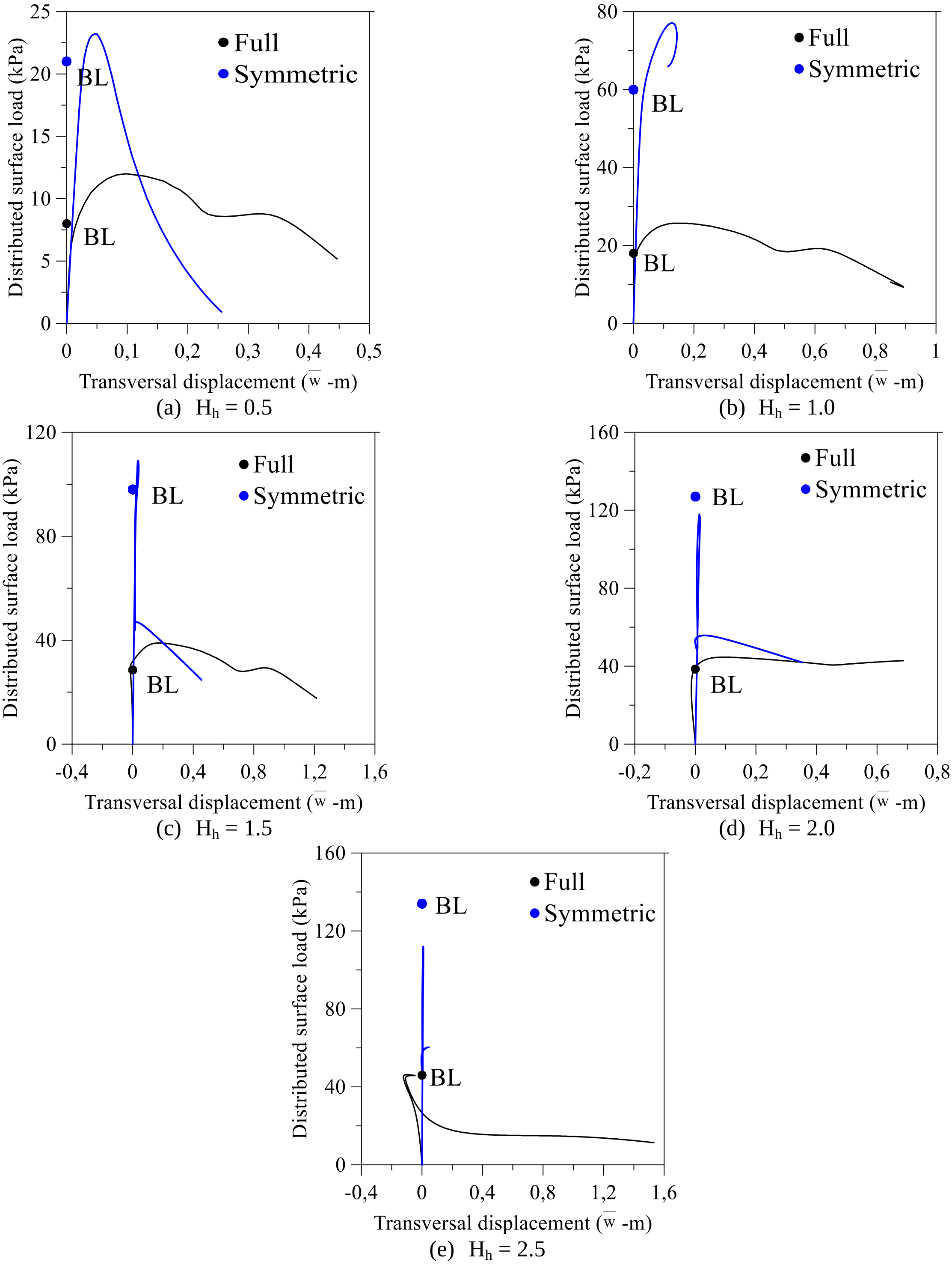

Figure 5. Nonlinear equilibrium paths for a simply-supported conoidal shell. Point $(x, y) = (3,0)$

Figure 6 shows the numerically obtained nonlinear frequency-amplitude relation associated with the lowest natural frequency. The nonlinear frequency-amplitude relation is obtained using the finite element software Abaqus® for the conoidal shell with simply-supported boundary conditions and H_h = 1.5m and H_h =2.0 *m*. To obtain this relation, a mesh with 1200 shell elements is used and the response is obtained for a node on the undeformed shell with the coordinates $(x, y) = (6, 2)$. A total of 7626 nonlinear equations of motion are numerically integrated, and the frequency – displacement relation is obtained using the methodology proposed by Nandakumar and Chatterjee (2005): the time response of the slightly damped system is obtained for a chosen node, and the maximum amplitude and corresponding period between two consecutive positive peaks are computed at each cycle. Consider two successive peaks at times T_1 and T_2. Let their average value be A_1 and the trough between these two positive peaks be A_2. The average amplitude can then be defined as $A = (A_1\text{-}A_2)/2$, and the corresponding frequency as $\omega = 1/(T_2\text{-}T_1)$. The scatter of points is due to the time step used in the FE analysis. The displacements (as in any time response) vary significantly near the peak and a very small integration time step is required in order to improve the results. This, of course, increases significantly the computation time. A typical time response used in the analysis is illustrated in Figure 7. The response shows a softening behavior which is due to the strong quadratic nonlinearity of the curved surface.

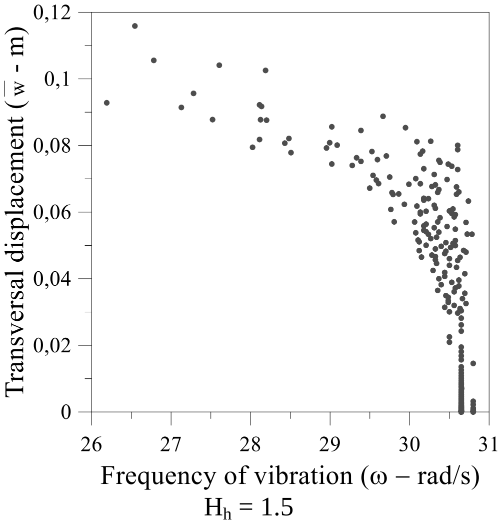

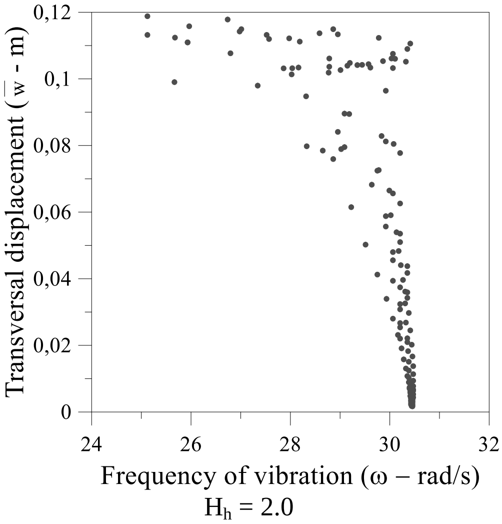

Figure 6. Frequency–amplitude relation. Transversal displacement $\overline{w}$ at the point $(x, y) = (6, 2)$.

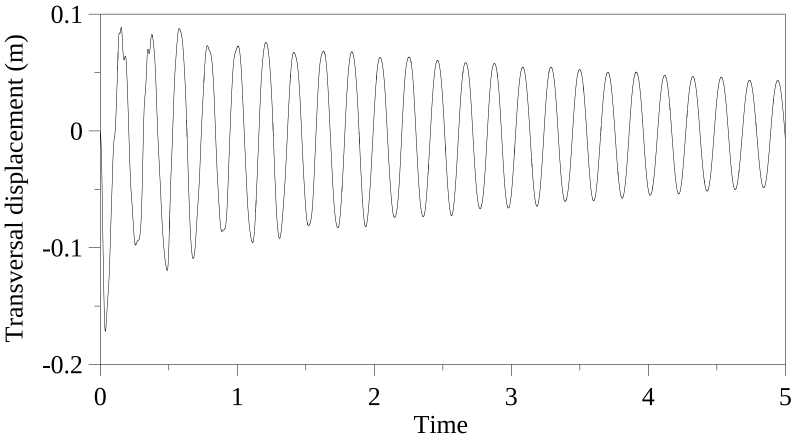

Figure 7. Time response. Nonlinear free damped vibrations. H_h =1.5m.

4. CONCLUDING REMARKS

The nonlinear formulation and finite element modeling using the finite element software Abaqus® of a shallow conoidal shell is presented in this paper. The results show the strong influence of the boundary conditions and geometry on the natural frequencies and buckling loads. The first vibration mode and buckling load is associated with an asymmetric mode. Thus the correct definition and appropriate choice of boundary conditions is necessary for a safe design. The shell displays a highly nonlinear response due to its strong quadratic and cubic nonlinearities. As the gravitational increases the effective stiffness decreases and becomes zero at a limit points where the shell loses its stability and a dynamic jump to an inverted equilibrium configuration occurs. The frequency-amplitude relation is of the softening type. This is due to the quadratic nonlinearity.

5. ACKNOWLEDGEMENTS

This work was made possible by the support of the Brazilian Ministry of Education –CNPq, FAPERJ-CNE and FAPEG.

6. REFERENCES

Balkshi, K. and Chakravorty, D., 2014. "First ply failure study of thin composite conoidal shells subjected to uniformly distributed load". *Thin-Walled Structures* Vol. 76, 1-7.

Brush, D.O. and Almroth,B. O., 1975. *Buckling of bars, plates and shells*. McGraw-Hill.

Cavalcanti, L.V. and Gonçalves, P.B., 2014. "Buckling and vibration analysis of conoidal shell roofs". In *Proceedings of the Symposium Shells, Membranes and Spatial Structures: Footprints - IASS-SLTE 2014*. Brasília, Brazil.

Cavalcanti, L.V., 2014. *Análise dinâmica, vibração e estabilidade de cascas conoidais abatidas*. Master thesis, Pontifícia Universidade Católica do Rio de Janeiro, Rio de Janeiro.

Das, A. K. and Bandyopadhyay, J. N., 1993. "Theoretical and experimental studies on conoidal shells". *Computers and. Structures*. Vol. 49, 531-536.

Ghosh, B. and Bandyopadhyay, J. N., 1990. "Approximate bending analysis of conoidal shells using the GalerkinMethod". *Computers and. Structures*. Vol. 36, 801-805.

Linkwitz, K., 1999. "About form finding of double-curved structures". *Engineering Structures.* Vol. 21(8), 709-718.

Nandakumar, K., Chatterjee, A., 2005. "Resonance, parameter estimation, and modal interactions in a strongly nonlinear Benchtop oscillator." *Nonlinear Dynamics*. Vol. 40, 149–167.

Nayak A.N. and Bandyopadhyay, J. N., 2002. "Free vibration analysis and design aids of stiffened conoidal shells". *Journal of Engineering Mechanics*/DOI: 10.1061/(ASCE)0733-9399(2002)128:4(419). 419-427.

Sahoo, S., 2013. "Dynamic characters of stiffened composite conoidal shell roofs with cutouts: design aids and selection guidelines". *Hindawi Publishing Corporation Journal of Engineering.* Vol. 2013 Article ID 230120.

Tisseur, F. and Meerbergen, K., 2001. "The quadratic eigenvalue problem", *SIAM Rev.*, Vol. 43, 235–286.

7. RESPONSIBILITY NOTICE

The author(s) is (are) the only responsible for the printed material included in this paper.